Environmental Science & Technology

pubs.acs.org/est

Article

Using High-Sensitivity Lipidomics To Assess Microscale Heterogeneity in Oceanic Sinking Particles and Single Phytoplankton Cells

Jonathan E. Hunter, Helen F. Fredricks, Lars Behrendt, Uria Alcolombri, Shavonna M. Bent, Roman Stocker, and Benjamin A. S. Van Mooy*

Cite This: *Environ. Sci. Technol.* 2021, 55, 15456−15465

Read Online

ACCESS | Metrics & More | Article Recommendations | Supporting Information

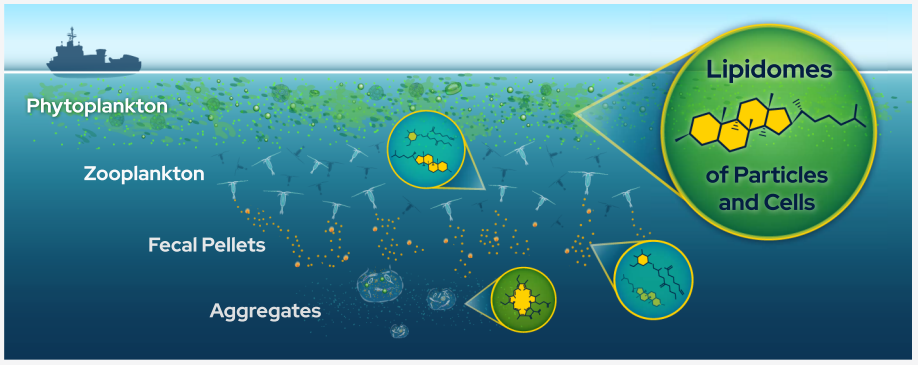

ABSTRACT: Sinking particulate organic matter (POM) is a primary component of the ocean's biological carbon pump that is responsible for carbon export from the surface to the deep sea. Lipids derived from plankton comprise a significant fraction of sinking POM. Our understanding of planktonic lipid biosynthesis and the subsequent degradation of lipids in sinking POM is based on the analysis of bulk samples that combine many millions of plankton cells or dozens of sinking particles, which averages out natural heterogeneity. We developed and applied a nanoflow high-performance liquid-chromatography electrospray-ionization high-resolution accurate-mass mass spectrometry lipidomic method to show that two types of sinking particles—marine snow and fecal pellets—collected in the western North Atlantic Ocean have distinct lipidomes, providing new insights into their sources and degradation that would not be apparent from bulk samples. We pressed the limit of this approach by examining individual diatom cells from a single culture, finding marked lipid heterogeneity, possibly indicative of fundamental mechanisms underlying cell division. These single-cell data confirm that even cultures of phytoplankton cells should be viewed as mixtures of physiologically distinct populations. Overall, this work reveals previously hidden lipidomic heterogeneity in natural POM and phytoplankton cells, which may provide critical new insights into microscale chemical and microbial processes that control the export of sinking POM.

KEYWORDS: *lipidomics, ocean, carbon export flux, particulate organic matter, marine snow, aggregate, fecal pellet, phytoplankton, single cell, nanoflow*

INTRODUCTION

Particulate organic matter (POM), derived primarily from plankton in the surface ocean, is ubiquitous in marine systems, and its fate is determined by microscale interactions with microbes.[1,2] Suspended POM spans both living planktonic cells and nonliving detrital material. A proportion of suspended POM is transformed by biological (e.g., zooplankton feeding) and physical processes (e.g., phytoplankton aggregation) into sinking POM, which is exported downward; this is a central component of the "biological carbon pump" and results in a flux of 4−13 Pg C year^{-1} from the surface to the deep ocean.[3,4] Thus, the biological pump is a substantive component of the global carbon cycle and a primary control on the Earth's climate.[5,6]

The overall efficiency of the biological carbon pump is governed by the sinking rate of particles and the rate of microbial degradation, which together act to attenuate the transmission of POM flux during its downward transit.[7] A disappearance of readily hydrolyzable organic matter is a characteristic transformation of POM.[8−10] Yet, studies of the

Received: April 30, 2021
Revised: October 12, 2021
Accepted: October 13, 2021
Published: November 1, 2021

chemical transformations that occur during POM production and processing are almost always observed by analysis of bulk samples; i.e., combining many hundreds of particles into a single sample masks particle-to-particle heterogeneity that could provide critical clues on the distributions of POM sources and degradation states. While sinking particles may be loosely characterized into three coarse categories—senescent single cells, fecal pellets from zooplankton, and aggregates of plankton cells (i.e., marine snow)[11]—few studies have attempted to differentiate them based on their chemical composition. The collection and analysis of bulk samples effectively homogenize and average the impacts of myriad microscale processes affecting the chemical composition of individual particles; these processes include direct respiration of POM by surface-associated microbes, microbial enzymatic or surfactant-mediated degradation and concomitant solubilization, mechanical disaggregation and zooplankton feeding, and subsequent feeding or heterotrophy on dissolved or suspended products thereof.[12] While it is generally accepted that these processes have different effects on the chemical composition of sinking particles, it is unlikely that all particles in a single bulk sample are affected in the same manner. For example, different types of sinking particles could have different susceptibilities to enzymatic degradation. Thus, variations in particle distributions in different samples could alone lead to concomitant differences in the degradation state of a bulk sample and, ultimately, predicted POM export flux dynamics. We suggest that elucidating the heterogeneous mechanistic linkages between the microscale physical and chemical processes that contribute to POM degradation on individual particles has the potential to improve our understanding of POM export.

Lipids are universal biomolecules with varied functions including acting as structural constituents in cellular membranes, energy storage reservoirs, and signals. Moreover, they represent an analytically tractable group of biomolecules to study in the context of marine POM.[13] Lipids comprise 10−30% of the carbon within plankton in the euphotic ocean[9,14] and therefore play an important role in the marine carbon cycle. We developed and employed a nanoflow high-performance liquid-chromatography electrospray-ionization high-resolution accurate-mass mass spectrometry (nano-HPLC/ESI HRAM MS) method for the characterization of lipids in individual sinking particles and in individual cells from which they are derived. Whether conceptual models of POM production and processing developed from bulk samples faithfully represent the actual processes that occur on the scales of cells and individual sinking particles is an open question. We describe a microscale analytical method that has the potential to answer it.

MATERIALS AND METHODS

Solvents and Standards. HPLC eluents were prepared from LC−MS grade isopropanol, water, and ammonium acetate (Fisher Scientific). LC−MS grade acetonitrile (Sigma) and formic acid (CovaChem) were also used for eluents. Sample makeup solvent also contained Milli-Q (Millipore) purity water. Borosilicate glassware was used for liquid handling and was precombusted at 450 °C overnight before use. The lipid standards used in this work and their origins are listed in Table S1.

Culturing and Single-Cell Isolation. *Thalassiosira weissflogii* strain CCMP1010, a 10−20 μm diameter centric diatom, was acquired from the NCMA culture collection (East Boothbay, ME, USA). Cultures were grown in L1 + Si enrichment media (Guillard and Hargraves, 1993) based on sterile filtered and autoclaved Sargasso seawater. After inoculation, a 25 mL batch culture was incubated at 18 °C, under a 14:10 h light/dark illumination cycle at 150 μmol m^{-2} s^{-1}. After 3 days of incubation, during exponential growth, a single culture was sampled for cell concentration determination by hemocytometer microscopy. The culture was diluted in fresh media to a concentration of 3 cells μL^{-1}. Next, precombusted 2 mL glass vials were treated with 2 mL of Milli-Q water and then dried gently under flowing N_2 to hydrate the surface and prevent droplet spreading. Finally, 0.3 μL droplets were pipetted into the base of the vials. Each vial was then visualized under brightfield illumination and chlorophyll autofluorescence on a Zeiss Axiostar upright microscope under 400× magnification. Vials containing exactly one cell were selected for extraction and analysis. Similarly, samples of multiple cells (10 to 12 cells) were diluted to approximately 10 cells μL^{-1}, confirmed by microscopy in 1 μL droplets, extracted, and analyzed.

Natural Particle Collection and Isolation. Sinking POM was collected from a single North Atlantic station during the AR16 cruise aboard the R/V *Neil Armstrong* between the 3rd and 22nd of May 2017. A surface-tethered, large-diameter net trap with a 0.2 μm mesh covered cod end[15] was deployed at 150 m for 24 h at approximately 32°7'N 64°23'W. At the end of the deployment, the trap was sealed remotely by acoustic release and recovered.

The particulate material collected in the cod end was suspended by gentle shaking, screened to remove particles and organisms of greater than 350 μm, and quantitatively split using an eight-way electronic rotating splitter.[16] Splits were allowed to settle at in situ temperature for 30 min in the dark, and the particulate material was aspirated into a Petri dish. The dense suspension was diluted with filtered seawater (0.2 μm poresize), and particles were hand-picked under a Zeiss Stemi 508 stereomicroscope using a 5 μL capillary. Picked particles were placed into a 96-well plate in a minimum volume (approximately 1−2 μL) of the seawater medium and imaged at 50× magnification, with the exception of very large marine snow type aggregates, which were imaged at 6.5×. An additional 5 μL of filtered seawater, collected in situ, was added to each well, and the plate was stored at −80 °C until extraction.

Lipid Micro-Extraction. In order to minimize the potential for the concentration of solvent contaminants, a microscale Bligh and Dyer extraction methodology[17] was developed as follows: samples were isolated in approximately 5 μL of aqueous media, either 0.22 μm filtered, in situ seawater (natural particles) or culture media (single cells). Extraction was performed in 2 mL glass vials by the addition of water (70 μL), dichloromethane (100 μL), and methanol (200 μL). Dinitrophenyl phosphatidylethanolamine (DNP-PE) internal standard (5.8 pmol) was added, and vials were sealed with PTFE-lined caps, vortexed, and sonicated for 5 min. Additional dichloromethane (100 μL) and water (100 μL) were added, and the samples were vortexed and centrifuged (100 × *g*, 5 min). Finally, the DCM lower phase was isolated using a 100 μL Hamilton syringe into a fresh 2 mL vial preloaded with the antioxidant butylated hydroxytoluene (1.5 nmol) and stored under an argon atmosphere at −20 °C.

https://doi.org/10.1021/acs.est.1c02836
Environ. Sci. Technol. 2021, 55, 15456−15465

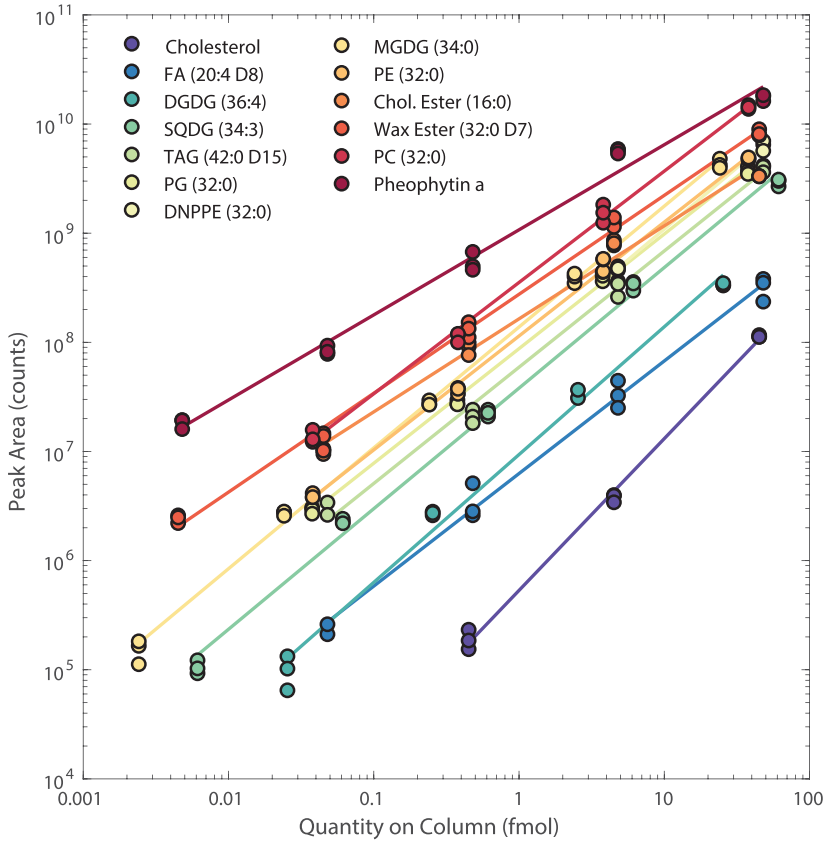

Figure 1. Calibration curves for the representative standards. Calibration coefficients and exponents for each lipid are given in Table S1, along with LOB, LOD, and LOQ results.

Nanoflow High-Performance Liquid Chromatography. Nanoflow high-performance liquid-chromatography (nano-HPLC) separation of marine lipids was carried out with a Thermo Scientific Easy nLC 1200 system. The flow path consisted of a direct injection on to a Thermo Scientific Acclaim PepMap 100 (75 μm × 2 cm; 3 μm; 100 Å), C18 guard column, and a Thermo Scientific Acclaim PepMap RSLC (75 μm × 15 cm; 2 μm; 100 Å) C18 analytical column, housed in a Phoenix S&T PST-BPH-20 butterfly column heater maintained at 50 °C.

Eluents comprised the following: Eluent A—75% water, 25% acetonitrile, 0.1% formic acid, and 0.04% ammonium hydroxide; Eluent B—75% isopropanol, 25% acetonitrile, 0.1% formic acid, and 0.04% ammonium hydroxide. The strong needle wash solvent was pure isopropanol, and the loading solvent and weak wash solvent were 95% water, 5% acetonitrile, and 0.1% formic acid. Finally, the samples were dissolved prior to analysis in 50% water and 50% isopropanol. The chromatographic gradient profile, at a constant flow rate of 300 nL min^{-1}, is defined in Table S2. Pressures were typically about 20 MPa.

High-Resolution Orbitrap Mass Spectrometry. The nano-HPLC system was coupled to a Thermo Scientific Q-Exactive orbitrap mass spectrometer via a Thermo Scientific Nanospray Flex source and stainless-steel emitter tip. A two-stage spray voltage was utilized to ensure optimal signal while ensuring a stable spray during the high-flow preequilibration and highly aqueous early gradient: the initial spray voltage, up to 25 min, was +2.4 and −1.9 kV followed by +2.1 and −1.9 kV until the end of the run, for positive and negative ion modes, respectively. Mass spectrometry conditions were as described by Hunter et al.[18]

Data processing, feature extraction, and annotation were performed using the LOBSTAHS[19] package as detailed in four previous studies from the WHOI laboratory: (1) intact polar diacylglycerolipids (IP-DAGs) and fatty acids (FAs);[20] (2) triacylglycerols (TAGs) and quinones;[21] (3) diacylglycerols (DAGs), sterols, sterol esters, and wax esters (WEs);[22] and (4) chloropigments and carotenoids.[23] We quantified different lipid classes using the ionization modes that were most sensitive; we used negative ionization data for fatty acids, while all other lipid classes were quantified by using positive ionization data. Six complete methodological blanks were used to subtract background signals in all of the samples of sinking POM. We observed that chlorophyll *a* was quantitatively transformed into pheophytin *a* prior to analysis, presumably due to the nature of the loading solvents; we report simply "pheophytin *a*", recognizing that, particularly in the diatom cells, chlorophyll *a* was likely the dominant contributor to this signal. None of the other lipid standards degraded. In our previous work on sterols and wax esters, we reported only summed concentrations for these two classes. Here, we venture to make putative assignments of several major sterols and wax esters based on their exact mass and retention time proximity to standards of closely related molecules (Table S3);[24,25] these criteria would equate to a Level 4 identification confidence in the scheme described by Schymanski et al.[26] We also confine our assignments to the major sterols in sinking particles with unique exact masses reported in the seminal work of Wakeham.[24] A typical lipid extract of a marine POM sample contains many hundreds of

https://doi.org/10.1021/acs.est.1c02836
Environ. Sci. Technol. 2021, 55, 15456−15465

lipids, but isotope-labeled internal standards are unavailable for all but a few dozen of these. Thus, all quantification was conducted by using external calibration curves of representative standards for each class of lipids (Table S1); we have shown previously that this approach yields quantitation that is statistically indistinguishable from the use of authentic isotope-labeled internal standards.[21] The limit of background (LOB), limit of detection (LOD), and limit of quantification (LOQ) were determined as prescribed by Armbruster and Pry (Table S1).[27]

Nonmetric multidimensional scaling (NMDS) analysis was conducted using the one hundred most abundant lipids (average relative abundance across samples) and the vegan package (version 2.5−7) in RStudio for R (version 4.0.3). The function metaMDS was utilized with the auto-transform function set to false. The R package ggplot2 was used for graphing of both NMDS plots. The calibration curves were graphed with MATLAB R2020a. We used Adobe Illustrator to unify the formats of these graphs in preparation for publication. Two-tailed t-tests were performed with Microsoft Excel and corrected for multiple comparisons using false discovery rate (FDR) calculation described by Benjamin and Hochberg.[28]

RESULTS AND DISCUSSION

Method Validation. We developed, tested, and applied a highly sensitive nano-HPLC/ESI HRAM MS lipidomic method specifically tuned to assess microscale POM heterogeneity in the ocean. Recent studies have shown that nano-HPLC/ESI HRAM MS methods are powerful tools for assessing the lipidomes of small samples from biological matrices,[29,30] but these methods have not yet been applied to natural marine particles or individual phytoplankton cells. Our nano-HPLC/ESI HRAM MS method yielded satisfactory separation and peak shapes for most of our analytical standards (Figure S1). The exception to this was our fatty acid standard, deuterated arachidonic acid (20:4 D8 FA), which was generally far from Gaussian in shape, particularly at higher concentrations. One possible explanation, albeit remote, is that the standard contained multiple stereoisomers. The FA standard also eluted considerably earlier than the others, indicating generally inefficient retention. The other standards showed average peak widths (full-width at half-maximum peak height) from 0.50 to 1.05 min (Table S1). The peak characteristics are in the same range as analytical-flow-rate HPLC/MS analyses of polar and neutral lipids in marine samples.[31,32]

We found that a power law ($y = Cx^a$) yielded the best fit to the standard calibration curves (Figure 1), where y is the peak area of the standards from their extracted ion chromatograms and x is the on-column quantity (fmol) of the standard. However, the average value of the exponent a was 1.05 ± 0.15, indicating a generally linear instrument response (Table S1), and thus, the coefficient C is effectively the linear response factor. The average R^2 was 0.994 ± 0.004, demonstrating excellent fits with the chosen function across the nearly five decades in on-column quantities we examined. The response factors varied by almost four orders of magnitude (Table S1). In positive ionization mode, the instrument response was the greatest for pheophytin *a* and the least for cholesterol. The order of response factors more or less followed the trend with the availability of polar groups in the molecules. However, the high response for wax esters and cholesterol esters was unexpected, since these molecules are nearly undetectable with the standard lipidomic ESI methods employed at the WHOI laboratory;[19,22] this observation exhibits the potential for unexpected gains in relative ionization efficiency from using nL min^{-1} flow rates.

Our goal for developing this nano-LC/ESI HRAM MS method was to achieve sensitivity sufficient for obtaining lipidomes of the POM in single particles collected from the ocean (Figure S2). The lowest predicted LOD values were for MGDG(34:0) and WE(32:0d7) at 0.01 fmol on-column. The highest LOD was for DNP-PE at 9.78 fmol on-column, which is a result of the high LOB (6.42 fmol on-column) for this analyte. We have used DNP-PE as an internal recovery standard in our laboratory for over a decade, and the levels in the blank analyses may suggest systematic low-level contamination or chromatographic carry-over. Cholesterol displays a similar relationship with LOD and LOB values of 4.07 and 2.74 fmol on-column, respectively. In addition to cholesterol, achievable detection for other lipids associated with human sebaceous excretions (free fatty acids and TAGs) was limited by blank levels. While all possible controls on lipid contamination, including using precombusted glassware and high grade solvents, were applied to this work, exhaustive steps are required to eliminate sources of lipid contamination and achieve the LODs afforded by the sensitivity of our nano-HPLC/ESI HRAM MS approach.[29,30]

The examples of DNP-PE and cholesterol notwithstanding, the LODs for most of the standards were in the 10−100 attomole on-column range, which is approximately two orders of magnitude more sensitive than recently described methods employing analytical-scale HPLC/MS (e.g., by Wörmer et al.[33]). Particulate concentrations of chlorophyll *a* and MGDG, common lipids in marine POM (e.g., Fulton et al.[34]), are on the order of 20 and 100 pmol L^{-1}, respectively, in the South Pacific subtropical gyre,[35] the most POM-depleted ocean waters in the world. Thus, our method would require samples of only approximately 0.1 microliters of this water for analysis in principle. In practice, water sampling, subsequent handling, and extraction could introduce contamination or other artifacts, preventing this sensitivity from being realized. Nonetheless, this calculation illustrates the potential frontiers that high-sensitivity lipidomic methods such as ours might open to the study of microscale POM processing.

Although our nano-HPLC/ESI HRAM MS method offers exquisite sensitivity, it does have some drawbacks. The hardware components are delicate and not forgiving to operators less familiar with their intricacies. We have also observed that retention times are less stable; combined with longer run times, unattended high-throughput operation is less feasible than with analytical-scale HPLC. Finally, in our experience with our specific application, we found that the spectrum of compatible solvent systems was narrower. In the end, we conceded the degradation of chlorophyll, one of our primary target analytes. In the absence of a necessity for high sensitivity, we caution that analytical-scale HPLC may still be a better choice for routine lipidomic analyses.

Lipidomic Analysis of Individual Sinking Particles. We applied our method to assess heterogeneity in the lipidomes of individual particles sinking through the upper mesopelagic zone of the western North Atlantic Ocean, examining both fecal pellets ($n = 20$) and marine snow ($n = 11$). It is essential to recognize that our approach of analyzing individual particles yields information that could not be obtained by pooling the two types of particles before extraction and analysis. First and

https://doi.org/10.1021/acs.est.1c02836
Environ. Sci. Technol. 2021, 55, 15456−15465

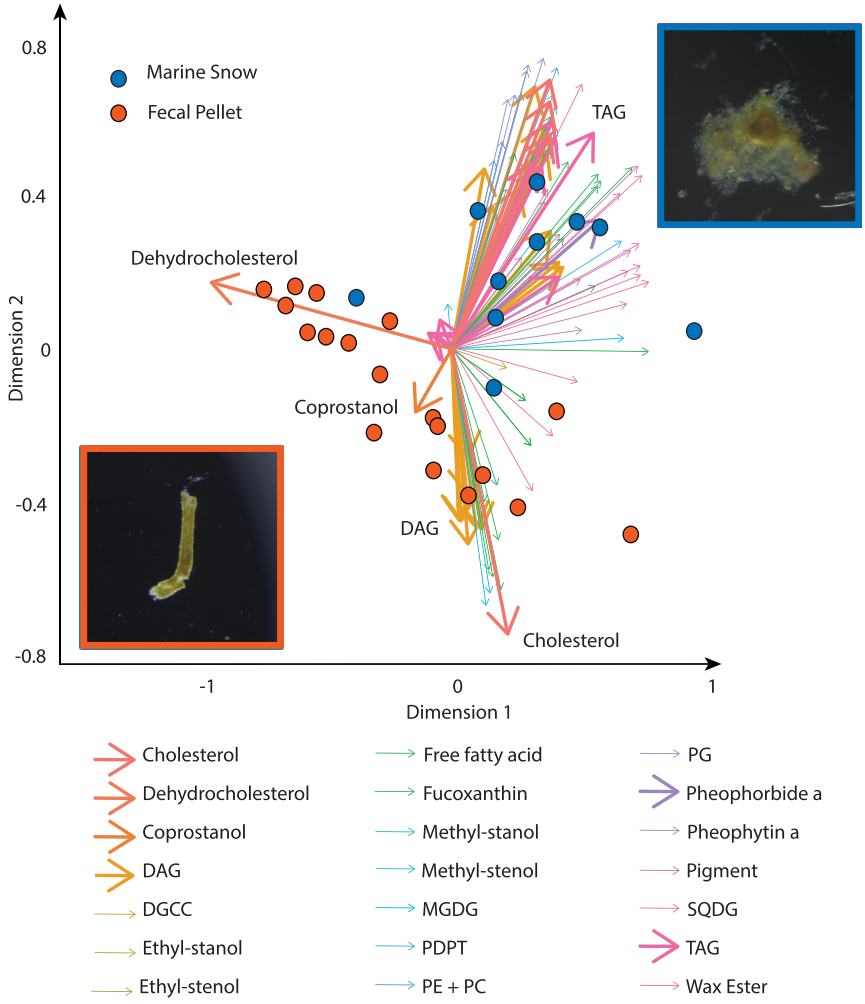

Figure 2. NMDS plot of lipidomes of individual marine snow particles and fecal pellets. Arrows indicate lipids that contributed significantly to the differences between samples; those mentioned in the text are highlighted by bold arrows. DAG = diaclyglycerols, MGDG = monogalactosyldiacylglycerols, DGCC = diacylglyceryl carboxyhydroxymethylcholine, PDPT = phosphatidyl-*S*,*S*-dimethylpropanethiols, PE + PC = phosphatidylethanolamines and phosphatidylcholines, PG = phosphatidylglycerols, SQDG = sulfoquinovosyldiacylglycerols, TAG = triacylglycerols. Pigments include carotenoids and minor chloropigments. Inset: photomicrographs of sinking fecal pellets and marine snow; the dimensions are approximately 5 mm × 5 mm.

foremost, the study's statistical power is lost because pooling results in a simple comparison of two bulk samples (n = 2). Therefore, this approach is not applicable for answering our questions about particle heterogeneity. In addition, as will be shown below, the fecal pellets and marine snow varied considerably in size. Thus, the pooled samples yield weighted averages that will be skewed by the largest and rarest sinking particles. In contrast, our approach provides single-particle lipidomic data that are largely independent of particle size. We maintain that examining individual particles can become a critical complement to analyses of bulk samples.

We found that total lipid content for fecal pellets ranged from 0.8 to 77 nmol C (particle)$^{-1}$, while marine snow contained 3.3 to 279 nmol C (particle)$^{-1}$. The range in the lipid content of these two types of individual particles highlights the dynamic range of the method and underscores their heterogeneity. We used microscopy to assess the average volume of the fecal pellets in separate samples (n = 85); the marine snow particles were too porous and poorly consolidated for such estimates. Assuming cylindrical geometry, we found that the volumes of the fecal pellets ranged from 0.06 to 3.59 mm^3 (particle)$^{-1}$. Using an average volume of 0.46 ± 0.29 mm^3 (particle)$^{-1}$ and the relationship between POC and volume (nmol C (mm)$^{-3}$)) compiled by Alldredge[36] for fecal aggregates, we estimate an organic carbon content of 53 ± 40 nmol C (particle)$^{-1}$. The average lipid content of fecal pellets was 14 ± 22 nmol C (particle)$^{-1}$, suggesting on average that about a quarter of the organic carbon in fecal pellets was from lipids. This estimate aligns very well with the findings of Wakeham et al.,[14] despite the uncertainties of our calculation and the large range in pellet size and lipid content.

We identified 531 individual lipids in at least 10 of the 31 sinking particles analyzed; 98 of these lipids were present in every particle. An NMDS analysis of the relative proportions of the 100 most abundant (average across all samples; Table S4) of these lipids showed that marine snow and fecal pellets' lipidomes were distinct, grouping separately from one another (Figure 2). The distance between the two groups was driven in part by the abundance of IP-DAGs and TAGs in the marine snow and DAGs in fecal pellets. Goutx et al.[37] used experiments in the Southern Ocean to define a lipolysis index based in part on these same molecules' distributions (FAs + DAGs)/(IP-DAGs + TAGs + WEs), which they argued was an indicator of the degradation stage of POC. We

https://doi.org/10.1021/acs.est.1c02836
Environ. Sci. Technol. 2021, 55, 15456−15465

calculated the lipolysis index of Goutx et al.[37] for both particle groups, finding average values of 0.7+/−0.2 and 1.8+/−1.5 for marine snow and fecal pellets (p = 0.02, t-test), suggesting that marine snow is less degraded. This is not a surprising outcome, since the POC in fecal pellets had passed through an animal's digestive tract. The NMDS also showed that sterols, particularly coprostanol and cholesterol, were important contributors to the separation of fecal pellets and marine snow into distinct groups. Interestingly, pheophorbide *a*, a molecule that has been used as a tracer of decaying organic matter for decades, was more strongly linked to marine snow than fecal pellets.

Importantly, the NMDS analysis also revealed that the heterogeneity of samples within both the marine snow and fecal pellet groups was almost as great as the heterogeneity between groups (Figure 2). We expected fecal pellets to be less heterogeneous than marine snow either because their original POM source would be narrow due to selective feeding by zooplankton or because zooplankton efficiently homogenize different POM sources during feeding and digestion. The coefficient of variation in the lipolysis index was 80%, indicating that the course of lipid degradation during POC digestion and subsequent sinking varied substantially between fecal pellets. Interestingly, a sterol with an m/z of 385.3461, indicating a molecular formula of $C_{27}H_{44}O$, appeared to drive the NMDS distance between different fecal pellet samples. We putatively assign this molecule as a dehydrocholesterol; both Gagosian et al.[38] and Wakeham and Canuel[39] reported 22-dehydrocholesterol as the second most abundant sterol in bulk samples of sinking particles, after cholesterol. Variability in putative dehydrocholesterol may reflect the different types of zooplankton that produced these pellets; this type of information could help us understand links between the zooplankton community structure and POM source and export. In the marine snow samples, the coefficient of variation for the lipolysis index was only 28%. Yet, IP-DAGs, carotenoids, and chloropigments drove considerable heterogeneity within the marine snow group (Figure 2). Carotenoids and pigments have been used for decades as chemotaxonic indicators; linking them to other single-particle data collected prior to lipid extraction (e.g., size and shape) could help ascertain connections between the phytoplankton community structure and sinking rate. Two marine snow samples appeared to group with the fecal pellets, suggesting that the proximate source of POM in these two samples was fecal pellets and not fresh phytoplankton cells. This shows that current approaches for visually distinguishing different particle types—important as they may be for categorizing physical properties affecting POM sinking speed and other parameters—may fall short in their ability to ascribe sources accurately.

The average quantities of the major lipid classes recapitulate differences in the relative variability in the individual lipids between marine snow and fecal pellets revealed in the NMDS analysis (Figure 3). However, it is essential to reiterate that these differences in averages would not be evident in samples of marine snow and fecal pellets pooled before analysis; our approach is unique because it is independent of particle size. Thus, each particle is weighted evenly when computing averages. Sterols contributed a 1.6+/−0.4 fold larger proportion of the lipids (t-test, p < 0.01, FDR-corrected) in the fecal pellets than the marine snow, 82+/−20% and 53+/−17% of the lipids, respectively. However, most of the other lipid classes were relatively more abundant in snow, including

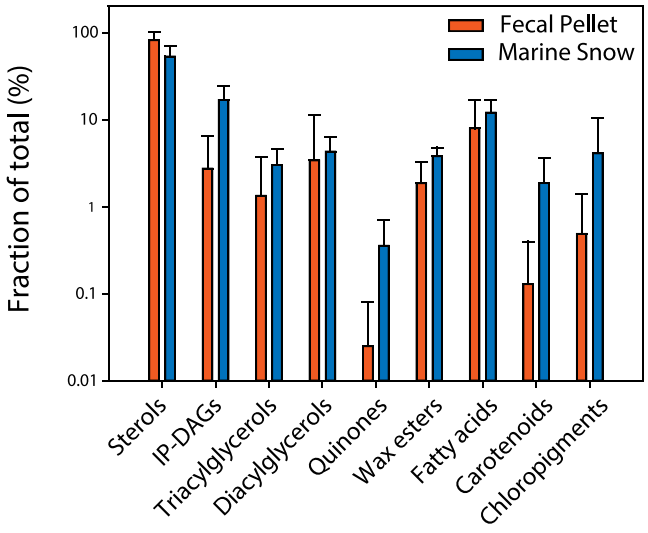

Figure 3. Fraction of marine snow particles and fecal pellets composed of the major lipid classes. IP-DAGs (intact polar diacylglycerolipids) are the sum of DGCC, digalactosyldiacylglycerols (DGDG), MGDG, PDPT, PC, PE, and PG.

IP-DAGs (t-test, p < 0.01, FDR-corrected), which are thought to reside primarily in living plankton and have been interpreted as a signal of relatively nondegraded POM. Obviously, the difference in sterol content alone affects these relative abundances to no small degree (Table S5). Furthermore, the response factors for different sterols analyzed by ESI-MS can vary widely,[40] and we used only a single sterol, cholesterol, for quantification of sterols. Yet even by removing sterols from the calculation and examining the relative abundance of lipids within the remaining fraction of the lipidome, IP-DAGs, chloropigments, carotenoids, and quinones are all more abundant in marine snow (t-test, p < 0.05, FDR-corrected; Table S4). This distribution of lipids reflects POM rich in fresh, and possibly still active, phytoplankton biomass. On the other hand, free fatty acids and wax esters are more abundant in fecal pellets (t-test, p < 0.05, FDR-corrected), reflecting degraded POM of zooplankton origin. This distinction between particle groups is consistent with the difference in the lipolysis index.

Our lipidomic analyses of individual marine snow particles and fecal pellets collected from sediment traps in the western North Atlantic Ocean show that there are significant differences between and within these two general classes of sinking POM. The lipids in sinking particles were of great interest in the 1980s and 1990s, but the available technology at the time (GC/MS) was not suited for assessing the true diversity of lipids—the lipidomes—in sinking particles.[9,13,41] As a result, the pace of new discoveries about POM export based on lipids has arguably slackened. Modern HPLC/HRAM MS methods are now approaching the goal of characterizing the entire lipidomes of marine particulate matter samples,[21,23,42] and our study demonstrates that nano-HPLC/ESI HRAM MS offers the sensitivity to differentiate particle-to-particle variations in lipid content.

Lipidomic Analysis of Single Cells. In order to explore even finer spatial scales of particle heterogeneity, we next turned our method toward assessing the lipidomes of individual diatom cells from a single culture. We chose to focus on the 34 most abundant lipids present in a bulk extract of *Thalassiosira weissflogii*, which is the set of lipids that each

https://doi.org/10.1021/acs.est.1c02836
Environ. Sci. Technol. 2021, 55, 15456−15465

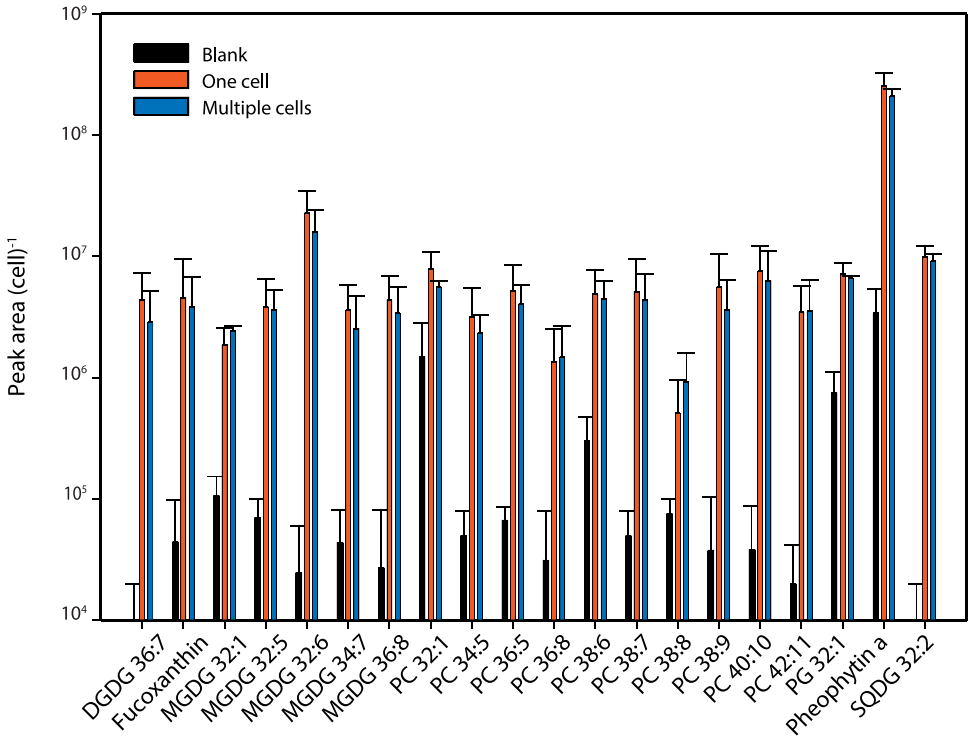

Figure 4. Raw peak area per-cell data for samples of single cells (1 cell; $n = 10$) and samples of multiple cells (10 to 12 cells; $n = 5$) from a single culture. Data are provided for the 20 lipids that are statistically distinct from the complete methodological blank and a signal-to-noise ratio greater than three. All of the TAGs and DAGs and many additional PCs and PGs failed to meet these criteria and were excluded. Note that the sum of the fatty acid chain length and unsaturation is provided for the IP-DAGs.

compose >1% of the lipidome by peak area. Together these lipid molecules accounted for about 80% of the total peak area. Of these 34 molecules, 20 met the dual criteria of being statistically distinct from the complete methodological blank (t-test, $p < 0.05$, FDR-corrected) and having a signal-to-noise ratio greater than three (Figure 4). Included in this group were pigments (pheophytin; fucoxanthin), glycolipids (MGDG, DGDG, and SQDG), and phospholipids (PC; Figure S3; Table S6). Acknowledging that these signals, though distinguishable from the background, were still quite small, we also assessed their quantitative accuracy in extracts from multiple cells (10 to 12 cells). The per-cell peak areas from the multicell extracts were indistinguishable from the peak areas of individual cells in all 20 cases (t-test, $p > 0.05$, FDR-corrected). This demonstrates both that the instrument response is linear across this range in signal intensity and that it is unlikely that background contamination was not accounted for by our methodological blanks. Thus, we interpret the heterogeneity in individual cells' lipid content as a valid indicator of cell-to-cell differences in physiological states.

We conducted an NMDS analysis to elucidate whether there were any systematic differences in the lipidomes of these cells (Figure 5). We found three groups of cells, suggesting different physiologically defined populations of cells in this single batch culture. Most of the separation between groups occurred along Dimension 1 and was driven in part by the pigments pheophytin *a* and fucoxanthin. This shows that the photophysiological status of individual cells varied markedly, even within a single culture. Due to the nature of the production of their siliceous frustule during miotic cell division, *T. weissflogii* produce daughter cells of two different sizes. As the cycle of cell division proceeds, cells of many distinct sizes may be present in a single culture, and this manifests as distinct populations of cells with different quantities of chlorophyll.[43] Our pheophytin and fucoxanthin results appear to recapitulate this. The physiological basis for variation along Dimension 2 is unknown but portends the potential for our approach for developing new hypotheses on cell-to-cell variability.

These single-cell data confirm that even axenic batch cultures of phytoplankton cells should be viewed as mixtures of physiologically distinct populations. This should leave no doubt that cells from individual strains in the same small volume of ocean water also have different lipidomes. Given that phytoplankton—primary producers in marine food webs—are the ultimate source of many classes of lipids in the ocean,[21,23] we must continue to vigilantly recognize that our current understanding of lipids in POM from bulk samples reflects the sum of myriad physiological variations in single cells.

In summary, we discovered fundamental differences in the composition of lipids in individual phytoplankton cells, marine snow particles, and fecal pellets and thereby elucidated microscale heterogeneity in the POM source and degradation state. The sinking of POM is the defining component of the biological carbon pump that regulates atmospheric carbon dioxide concentrations. Fundamentally, the balance of degradation rates and sinking velocities of individual cells and particles defines the fraction of sinking POM that reaches abyssal depths. The lipid composition affects both of these rates; e.g., different lipid molecules have structurally defined susceptibilities to various degradation processes,[44] and lipids are negatively buoyant in seawater, affecting particle density and thereby sinking speed.[45] The potential future power of our approach will be to establish connections between lipids,

https://doi.org/10.1021/acs.est.1c02836
Environ. Sci. Technol. 2021, 55, 15456−15465

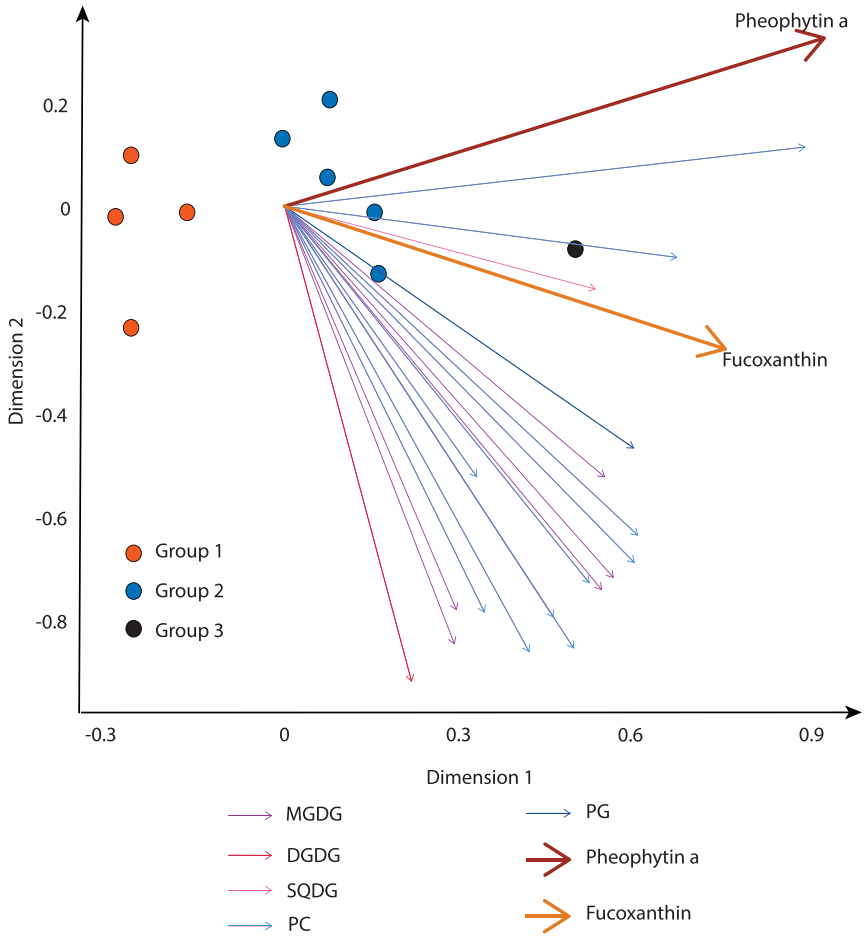

Figure 5. NMDS plot of lipidomes of the individual *T. weissflogii* cells (1 cell, $n = 10$), based on the same lipid molecules given in Figure 4. Arrows indicate lipids that contributed significantly to the differences between samples; bold arrows highlight those mentioned in the text.

degradation rates, and sinking velocities at the microscale. New conceptual frameworks, e.g., those that incorporate microscale physics or advanced imaging data, will need to be developed for this purpose. They are urgently needed to improve our current understanding of the biological pump's potential response to future global warming.

■ ASSOCIATED CONTENT

Supporting Information

The Supporting Information is available free of charge at https://pubs.acs.org/doi/10.1021/acs.est.1c02836.

(Tables S1−S6 and Figures S1−S3) Performance characteristics for the nano-HPLC/ESI HRAM MS method; chromatographic gradient profile over the course of the 100 min analysis; sterols and wax esters that were putatively identified by nano-HPLC/ESI HRAM MS; nano-HPLC/ESI HRAM MS data used for identification of the top 100 lipids in individual sinking particles; average lipid composition of sinking fecal pellets and marine snow particles; nano-HPLC/ESI HRAM MS data used for identification of the top 20 lipids in single *T. weissflogii* cells; extracted ion chromatograms for the lipid standards; and extracted ion chromatograms from single cells (PDF)

■ AUTHOR INFORMATION

Corresponding Author

Benjamin A. S. Van Mooy − *Marine Chemistry and Geochemistry, Woods Hole Oceanographic Institution, Woods Hole, Massachusetts 02543-1050, United States;* orcid.org/0000-0002-2804-6508; Email: bvanmooy@whoi.edu

Authors

Jonathan E. Hunter − *Marine Chemistry and Geochemistry, Woods Hole Oceanographic Institution, Woods Hole, Massachusetts 02543-1050, United States;* Present Address: Sport and Specialized Analytical Services, LGC, Fordham, Cambridgeshire CB7 5WW, U.K. (J.E.H.)

Helen F. Fredricks − *Marine Chemistry and Geochemistry, Woods Hole Oceanographic Institution, Woods Hole, Massachusetts 02543-1050, United States*

Lars Behrendt − *Institute of Environmental Engineering, Department of Civil, Environmental and Geomatic Engineering, ETH Zürich, Zürich 8093, Switzerland;* Present Address: Department of Organismal Biology, Science for Life Laboratory, Uppsala University, Norbyvägen 18A, Uppsala 75236, Sweden (L.B.)

Uria Alcolombri − *Institute of Environmental Engineering, Department of Civil, Environmental and Geomatic Engineering, ETH Zürich, Zürich 8093, Switzerland*

https://doi.org/10.1021/acs.est.1c02836
Environ. Sci. Technol. 2021, 55, 15456−15465

Shavonna M. Bent − *Marine Chemistry and Geochemistry, Woods Hole Oceanographic Institution, Woods Hole, Massachusetts 02543-1050, United States*
Roman Stocker − *Institute of Environmental Engineering, Department of Civil, Environmental and Geomatic Engineering, ETH Zürich, Zürich 8093, Switzerland*

Complete contact information is available at: https://pubs.acs.org/10.1021/acs.est.1c02836

Author Contributions

J.E.H. collected all of the data reported in this manuscript. H.F.F. assisted with methodological development and validation. S.M.B. contributed data analysis. L.B. and U.A. assisted in the study design and in carrying out the collection of samples in the field. B.A.S.V.M. and R.S. designed and oversaw the study. J.E.H. and B.A.S.V.M. co-wrote the initial manuscript draft, and all other authors contributed substantively to the final version.

Notes

The authors declare no competing financial interest.

■ ACKNOWLEDGMENTS

We thank Daniel Lowenstein (WHOI) for assistance with sterol mass spectrum interpretation. L.M.B. was supported by grants from the Science for Life Laboratory. The research cruise aboard the R/V *Neil Armstrong* was supported by the National Science Foundation (OCE-1536346). R.S. acknowledges support from a Symbiosis in Aquatic Systems Investigator Award from the Gordon and Betty Moore Foundation (GBMF9197). This research was funded by a grant from the Marine Microbiology Initiative division of the Gordon and Betty Moore Foundation (GBMF5073 to B.A.S.V.M. and R.S.). This work was supported by a grant from the Simons Foundation and is a contribution of the Simons Collaboration on Ocean Processes and Ecology (SCOPE; #721229 to B.A.S.V.M.).

■ REFERENCES

(1) Azam, F. Microbial control of oceanic carbon flux: the plot thickens. *Science* **1998**, *280*, 694−696.
(2) Stocker, R. Marine Microbes See a Sea of Gradients. *Science* **2012**, *338*, 628−633.
(3) Lima, I. D.; Lam, P. J.; Doney, S. C. Dynamics of particulate organic carbon flux in a global ocean model. *Biogeosciences* **2014**, *11*, 1177−1198.
(4) Honjo, S.; Eglinton, T. I.; Taylor, C. D.; Ulmer, K. M.; Sievert, S. M.; Bracher, A.; German, C. R.; Edgcomb, V.; Francois, R.; Iglesias-Rodriguez, M. D.; van Mooy, B.; Rapeta, D. Understanding the Role of the Biological Pump in the Global Carbon Cycle: An Imperative for Ocean Science. *Oceanography* **2014**, *27*, 10−16.
(5) Sanders, R.; Henson, S. A.; Koski, M.; De La Rocha, C. L.; Painter, S. C.; Poulton, A. J.; Riley, J.; Salihoglu, B.; Visser, A.; Yool, A.; Bellerby, R.; Martin, A. P. The Biological Carbon Pump in the North Atlantic. *Prog. Oceanogr.* **2014**, *129*, 200−218.
(6) Kwon, E. Y.; Primeau, F.; Sarmiento, J. L. The impact of remineralization depth on the air-sea carbon balance. *Nat. Geosci.* **2009**, *2*, 630−635.
(7) Martin, J. H.; Knauer, G. A.; Karl, D. M.; Broenkow, W. W. VERTEX: carbon cycling in the northeast Pacific. *Deep Sea Res. Part A Oceanogr. Res. Pap.* **1987**, *34*, 267−285.
(8) Goutx, M.; Wakeham, S. G.; Lee, C.; Duflos, M.; Guigue, C.; Liu, Z.; Moriceau, B.; Sempére, R.; Tedetti, M.; Xue, J. Compostion and degradation of marine particles with different settling velocities in the northwestern mediterranean sea. *Limnol. Oceanogr.* **2007**, *52*, 1645−1664.
(9) Wakeham, S. G.; Lee, C.; Hedges, J. I.; Hernes, P. J.; Peterson, M. L. Molecular indicators of diagenetic status in marine organic matter. *Geochim. Cosmochim. Acta* **1997**, *61*, 5363−5369.
(10) Van Mooy, B. A. S.; Keil, R. G.; Devol, A. H. Impact of suboxia on sinking particulate organic matter: enhanced carbon flux and preferential degradation of amino acids via denitrification. *Geochim. Cosmochim. Acta* **2002**, *66*, 457−465.
(11) Durkin, C. A.; van Mooy, B. A. S.; Dyhrman, S. T.; Buesseler, K. O. Sinking phytoplankton associated with carbon flux in the Atlantic Ocean. *Limnol. Oceanogr.* **2016**, *61*, 1172−1187.
(12) Collins, J. R.; Edwards, B. R.; Thamatrakoln, K.; Ossolinski, J. E.; DiTullio, G. R.; Bidle, K. D.; Doney, S. C.; Van Mooy, B. A. S. The multiple fates of sinking particles in the North Atlantic Ocean. *Global Biogeochem. Cycles* **2015**, *29*, 1471−1494.
(13) Wakeham, S. G.; Farrington, J. W.; Gagosian, R. B.; Lee, C.; DeBaar, H.; Nigrelli, G. E.; Tripp, B. W.; Smith, S. O.; Frew, N. M. Organic matter fluxes from sediment traps in the equatorial Atlantic Ocean. *Nature* **1980**, *286*, 798−800.
(14) Wakeham, S. G.; Hedges, J. I.; Lee, C.; Peterson, M. L.; Hernes, P. J. Compositions and transport of lipid biomarkers through the water column and surficial sediments of the equatorial Pacific Ocean. *Deep-Sea Res. II* **1997**, *44*, 2131−2162.
(15) Peterson, M. L.; Hernes, P. J.; Thoreson, D. S.; Ifedges, J. I.; Lee, C.; Wakeham, S. G. Field evaluation of a valved sediment trap. *Limnol. Oceanogr.* **1993**, *38*, 1741−1761.
(16) Lamborg, C. H.; Buesseler, K. O.; Valdes, J. R.; Bertrand, C. H.; Bidigare, R.; Manganini, S.; Pike, S.; Steinberg, D.; Trull, T.; Wilson, S. The flux of bio- and litho-genic material associated with sinking particles in the mesopelagic "twilight zone" of the Northwest and North Central Pacific Ocean. *Deep Sea Res. Part II: Top. Stud. Oceanogr.* **2008**, *55*, 1540−1563.
(17) Bligh, E. G.; Dyer, W. J. A rapid method of total lipid extraction and purification. *Can. J. Biochem. Physiol.* **1959**, *37*, 911−917.
(18) Hunter, J. E.; Frada, M. J.; Fredricks, H. F.; Vardi, A.; van Mooy, B. A. S., *Targeted and Untargeted Lipidomics of Emiliania huxleyi Viral Infection and Life Cycle Phases Highlights Molecular Biomarkers of Infection, Susceptibility, and Ploidy*. Front. Mar. Sci. 2015, DOI: 10.3389/fmars.2015.00081.
(19) Collins, J. R.; Edwards, B. R.; Fredricks, H. F.; Van Mooy, B. A. S. LOBSTAHS: An adduct-based lipidomics strategy for discovery and identification of oxidative stress biomarkers. *Anal. Chem.* **2016**, *88*, 7154−7162.
(20) Collins, J. R.; Fredricks, H. F.; Bowman, J. S.; Ward, C. P.; Moreno, C.; Longnecker, K.; Marchetti, A.; Hansel, C. M.; Ducklow, H. W.; Van Mooy, B. A. S. The molecular products and biogeochemical significance of lipid photooxidation in West Antarctic surface waters. *Geochim. Cosmochim. Acta* **2018**, *232*, 244−264.
(21) Becker, K. W.; Collins, J. R.; Durham, B. P.; Groussman, R. D.; White, A. E.; Fredricks, H. F.; Ossolinski, J. E.; Repeta, D. J.; Carini, P.; Armbrust, E. V.; Van Mooy, B. A. S. Daily changes in phytoplankton lipidomes reveal mechanisms of energy storage in the open ocean. *Nat. Commun.* **2018**, *9*, 5179.
(22) Miller, C. A.; Holm, H. C.; Horstmann, L.; George, J. C.; Fredricks, H. F.; van Mooy, B. A. S.; Apprill, A. Coordinated transformation of the gut microbiome and lipidome of bowhead whales provides novel insights into digestion. *ISME J.* **2020**, *14*, 688−701.
(23) Becker, K. W.; Harke, M. J.; Mende, D. R.; Muratore, D.; Weitz, J. S.; DeLong, E. F.; Dyhrman, S. T.; van Mooy, B. A. S. Combined pigment and metatranscriptomic analysis reveals highly synchronized diel patterns of phenotypic light response across domains in the open oligotrophic ocean. *ISME J.* **2021**, *15*, 520−533.
(24) Wakeham, S. G. Reduction of stenols to stanols in particulate matter at oxic−anoxic boundaries in sea water. *Nature* **1989**, *342*, 787−790.

(25) Wakeham, S. G. Wax esters and triacylglycerols in sinking particulate matter in the Peru upwelling area (15°S, 75°W). *Mar. Chem.* **1985**, *17*, 213−235.
(26) Schymanski, E. L.; Jeon, J.; Gulde, R.; Fenner, K.; Ruff, M.; Singer, H. P.; Hollender, J., *Identifying small molecules via high resolution mass spectrometry: communicating confidence*; ACS Publications: 2014.
(27) Armbruster, D. A.; Pry, T. Limit of blank, limit of detection and limit of quantitation. *Clin. Biochem. Rev.* **2008**, *29*, S49.
(28) Benjamini, Y.; Hochberg, Y. Controlling the false discovery rate: a practical and powerful approach to multiple testing. *J. R. Stat. Soc. Ser. B (Methodol.)* **1995**, 289−300.
(29) Liu, P.; Corilo, Y. E.; Marshall, A. G. Polar lipid composition of biodiesel algae candidates Nannochloropsis oculata and Haematococcus pluvialis from nano liquid chromatography coupled with negative electrospray ionization 14.5 T Fourier transform ion cyclotron resonance mass spectrometry. *Energy Fuels* **2016**, *30*, 8270−8276.
(30) Danne-Rasche, N.; Coman, C.; Ahrends, R. Nano-LC/NSI MS refines lipidomics by enhancing lipid coverage, measurement sensitivity, and linear dynamic range. *Anal. Chem.* **2018**, *90*, 8093−8101.
(31) Wörmer, L.; Lipp, J. S.; Schröder, J. M.; Hinrichs, K.-U. Application of two new LC−ESI−MS methods for improved detection of intact polar lipids (IPLs) in environmental samples. *Org. Geochem.* **2013**, *59*, 10−21.
(32) Hopmans, E. C.; Schouten, S.; Sinninghe Damsté, J. S. The effect of improved chromatography on GDGT-based palaeoproxies. *Org. Geochem.* **2016**, *93*, 1−6.
(33) Wörmer, L.; Lipp, J. S.; Hinrichs, K.-U. Comprehensive analysis of microbial lipids in environmental samples through HPLC-MS protocols. *Hydrocarbon and Lipid Microbiology Protocols: Petroleum, Hydrocarbon and Lipid Analysis* 2017, 289 −317.
(34) Fulton, J. M.; Fredricks, H. F.; Van Mooy, B. A. S. Intact polar lipid export in the temperate western North Atlantic and Sargasso Sea. *Org. Geochem.* **2017**, *114*, 45−56.
(35) Van Mooy, B. A. S.; Fredricks, H. F. Bacterial and eukaryotic intact polar lipids in the eastern subtropical South Pacific: water-column distribution, planktonic sources, and fatty acid composition. *Geochim. Cosmochim. Acta* **2010**, *74*, 6499−6516.
(36) Alldredge, A. The carbon, nitrogen and mass content of marine snow as a function of aggregate size. *Deep Sea Res. Part I: Oceanogr. Res. Pap.* **1998**, *45*, 529−541.
(37) Goutx, M.; Guigue, C.; Striby, L. Triacylglycerol biodegradation experiment in marine environmental conditions: definition of a new lipolysis index. *Org. Geochem.* **2003**, *34*, 1465−1473.
(38) Gagosian, R.; Volkman, J.; Nigrelli, G., The use of sediment traps to determine sterol sources in coastal sediments off Peru. In *Advances in Organic Geochemistry 1981*; Wiley Chichester: 1981, 369−379.
(39) Wakeham, S. G.; Canuel, E. A. Organic geochemistry of particulate matter in the eastern tropical North Pacific Ocean: Implications for particle dynamics. *J. Mar. Res.* **1988**, *46*, 183−213.
(40) McDonald, J. G.; Thompson, B. M.; McCrum, E. C.; Russell, D. W. Extraction and analysis of sterols in biological matrices by high performance liquid chromatography electrospray ionization mass spectrometry. *Methods Enzymol.* **2007**, *432*, 145−170.
(41) Mayzaud, P.; Chanut, J. P.; Ackman, R. G. Seasonal changes of the biochemical composition of marine particulate matter with special reference to fatty acids and sterols. *Mar. Ecol. Prog. Ser.* **1989**, *56*, 189−204.
(42) Cantarero, S. I.; Henríquez-Castillo, C.; Dildar, N.; Vargas, C. A.; Von Dassow, P.; Cornejo-D'Ottone, M.; Sepúlveda, J. Size-fractionated contribution of microbial biomass to suspended organic matter in the eastern Tropical South Pacific oxygen minimum zone. *Front. Mar. Sci.* **2020**, *7*, 745.
(43) Armbrust, E. V.; Chisholm, S. W.; Olson, R. J. Role of light and the cell cycle on the induction of spermatogenesis in a centric diatom. *J. Phycol.* **1990**, *26*, 470−478.
(44) Rontani, J. F.; Zabeti, N.; Wakeham, S. G. Degradation of particulate organic matter in the equatorial Pacific Ocean: Biotic or abiotic? *Limnol. Oceanogr.* **2011**, *56*, 333−349.
(45) Wakeham, S. G.; Cowen, J. P.; Burd, B. J.; Thomson, R. E. Lipid-rich ascending particles from the hydrothermal plume at Endeavour Segment, Juan de Fuca Ridge. *Geochim. Cosmochim. Acta* **2001**, *65*, 923−939.

https://doi.org/10.1021/acs.est.1c02836
Environ. Sci. Technol. 2021, 55, 15456−15465